ARMY RESEARCH LABORATORY

Investigation of the Effect of Various Oxide and Flouride Additives on the Microstructure, Electronic Properties, and Phase Shifting Ability of $Ba_{1-x}Sr_xTiO_3$

L.C. Sengupta, E. Ngo, S. Stowell, R. Lancto, W.C. Drach,
T.E. Koscica, and R.W. Babbitt

ARL-TR-217 September 1993

The findings in this report are not to be construed as an official Department of the Army position unless so designated by other authorized documents.

Citation of manufacturer's or trade names does not constitute an official endorsement or approval of the use thereof.

Destroy this report when it is no longer needed. Do not return it to the originator.

REPORT DOCUMENTATION PAGE

Form Approved
OMB No. 0704-0188

1. AGENCY USE ONLY (Leave blank)	2. REPORT DATE	3. REPORT TYPE AND DATES COVERED
	September 1993	Final Report

4. TITLE AND SUBTITLE
Investigation of the Effect of Various Oxide and Fluoride Additives on the Microstructure, Electronic Properties, and Phase Shifting Ability of $Ba_{1-x}Sr_xTiO3$

5. FUNDING NUMBERS

6. AUTHOR(S)
L. C. Sengupta, E. Ngo, S. Stowell, and R. Lancto
W. C. Drach,* T. E. Koscica,* and R. W. Babbitt*

7. PERFORMING ORGANIZATION NAME(S) AND ADDRESS(ES)
U.S. Army Research Laboratory
Watertown, MA 02172-0001
ATTN: AMSRL-MA-CA

8. PERFORMING ORGANIZATION REPORT NUMBER
ARL-TR-217

9. SPONSORING/MONITORING AGENCY NAME(S) AND ADDRESS(ES)
U.S. Army Research Laboratory
2800 Powder Mill Road
Adelphi, MD 20783-1145

10. SPONSORING/MONITORING AGENCY REPORT NUMBER

11. SUPPLEMENTARY NOTES
*U.S. Army Research Laboratory
Fort Monmouth, NJ 07703
ATTN: AMSRL-EP-M

12a. DISTRIBUTION/AVAILABILITY STATEMENT
Approved for public release; distribution unlimited.

12b. DISTRIBUTION CODE

13. ABSTRACT (Maximum 200 words)

A ceramic phase shifting device (used in phased array antenna systems) has been demonstrated using $Ba_{1-x}Sr_xTiO_3$ (BSTO) ceramics. As a part of an effort to optimize the electronic device performance in the phase shifter, various dopants have been incorporated into BSTO. The effects of these additives on the Curie temperature, dielectric properties, tunability, hysteresis, and grain size have been investigated. The homogeneity of the doped materials has been verified using Curie-Weiss analysis. To further improve the electrical performance, some higher levels of doping have been attempted. A few of the latest results for these ceramic-ceramic composites will be presented.

14. SUBJECT TERMS	15. NUMBER OF PAGES
Phased array antennas, Ferroelectrics, Electro-ceramics, Barium stronitum titanate	26
	16. PRICE CODE

17. SECURITY CLASSIFICATION OF REPORT	18. SECURITY CLASSIFICATION OF THIS PAGE	19. SECURITY CLASSIFICATION OF ABSTRACT	20. LIMITATION OF ABSTRACT
Unclassified	Unclassified	Unclassified	UL

Contents

Figures

Tables

Introduction

Phased array antennas can steer the transmitted or received signals either linearly or in two dimensions without mechanical oscillation. These antennas are currently constructed using ferrite phase shifting elements. Due to the type of circuit requirements necessary to operate these antennas, they are costly, large, and heavy; therefore, their use has been limited primarily to strategically depentent military applications. In order to make these devices available for many other commercial and military uses, the basic concept of the antenna must be improved. If ferroelectric material could be used instead of ferrites, phased array antennas would be totally revolutionized.

The concept of using ferroelectric materials for phased array radar systems is not new. However, due to new and sophisticated device fabrication and testing, as well as to the advent of new improvements in electro-ceramic formulations and ceramic processing, the use of these materials seems more realistic than ever.

A ceramic barium strontium titanate (BSTO), $Ba_{1-x}Sr_xTiO_3$, electro-optic phase shifter using a planar microstrip construction has been demonstrated (1). In order to meet the required performance specifications for maximum phase shifting ability, the electronic properties in the low frequency (KHz) and microwave regions (GHz) must be optimized. As part of this optimization process various dopants have been added to the material and their effects on the electronic properties have been studied. The relationships between the effect of these dopants on the dielectric constants, tunability, grain size, Curie temperature and, in some cases, strontium content have been investigated and will be discussed in this report. This report will outline some of the initial findings and compare the results found for some of the dopants to the results obtained in doped $BaTiO_3$ (BTO).

Experimental

Ceramic Processing

Table 1 contains the additives, sample numbers, calcining, and sintering temperatures for the specimens examined in this investigation. Various oxide and fluoride additives were mixed with $BaTiO_3$ (Ferro Corp. #219-6) and $SrTiO_3$ (Ferro Corp. #218) in a formulation for additive testing of $Ba_{0.75}Sr_{0.25}TiO_3$. The mixture was ball milled in ethanol using alumina grinding media for about 24 hours and subsequently air dried. The powder is then calcined at the temperatures given in Table 1. The calcined material was then made into a slurry with ethanol and ball milled with alumina grinding media for 24 hours. At this time, 3 wt% organic binder from Rohm and Haas Company, product Rhoplex B-60A which is an aqueous emulsion of acrylic polymer, was added to improve green body strength and permit sample fabrication. The mixture was then ball milled for another four to five hours and air dried. The powder was cold uniaxially pressed at a pressure of approximately 7000 psi. The pellets were sintered at the temperatures given in Table 1 for an average soak time of about two hours. Table 2 gives the final geometrical densities, % theoretical density, % porosity (open) and % liquid absorption (ethanol) for the specimens listed in Table 1. The % porosity and the % liquid absorption were determined from immersion density methods, using specimens which were placed in a vacuum and then saturated with ethanol; the % porosity was determined from the dry weight, the saturated weight, and the suspended (in ethanol) saturated weights.

Table 1. Sample descriptions of doped BSTO (Ba=0.75) and $BaTiO_3$

Sample #	Additive	Calcining temp. (°C)	Sintering temp. (°C)
BSTO			
A30	1 wt% ZrO_2	1100	1325
A31	1 wt% ZrO_2, 1 wt% $BaLiF_3$	700	1335
A32	5 m% $Bi_2(SnO_3)_3$	1100	1350
A33	5 m% $Bi_2(SnO_3)_3$, 1 wt% $BaLiF_3$	700	1335
A35	1.8 wt% $CaSnO_3$	1100	1325
A36	2 wt% $CaTiO_3$	1100	1325
A37	2 m% $NiSnO_3$	1100	1350
A38	2.5 wt% $BaLiF_3$, CaO, MnO_2	700	1325
A39	1 wt% Al_2O_3	1100	1335
A40	30 wt% Al_2O_3	1100	1335
A68	Undoped	1100	1335
$BaTiO_3$			
A58	1 wt% ZrO_2 , 1 wt% $BaLiF_3$	700	1335
A59	5 m% $Bi_2(SnO_3)_3$	1100	1335
A60	30 wt% Al_2O_3	1100	1335
A61	1 wt% Al_2O_3	1100	1335
A62	2.5 wt% $BaLiF_3$, CaO, MnO_2	700	1350
A63	2 m% $NiSnO_3$	1100	1350
A64	2 wt% $CaTiO_3$	1100	1325
A65	6 wt% $CaTiO_3$, 4 wt% $CaSnO_3$	1100	1350
A66	2 m% $CaSnO_3$	1100	1325
A67	5 m% Bi2$(SnO_3)_3$, 1 wt% $BaLiF_3$	700	1335
A69	Undoped	1100	1335

Table 2. Densities and porosity of doped BSTO (Ba=0.75) and doped $BaTiO_3$

Sample #	Density (g/cm^3)	% Theoretical density	% Porosity	% Liquid absorption
BSTO				
A30	5.44	96	2.31	0.34
A31	5.13	91	5.58	0.84
A32	5.22	92	2.25	0.33
A33	5.19	91	2.54	0.36
A35	5.32	94	1.01	0.15
A36	5.14	91	9.15	1.45
A37	5.20	92	2.41	0.35
A38	5.11	90	2.48	0.36
A39	5.20	92	2.36	0.36
A40	3.97	–	6.76	1.44
A68	5.54	97	0.62	0.08
$BaTiO_3$				
A58	5.49	94	5.95	0.88
A59	5.79	99	3.95	0.54
A60	3.40	–	17.82	4.02
A61	5.22	90	4.96	0.80
A62	5.13	88	20.12	3.35
A63	5.97	100	3.69	0.55
A64	5.32	91	6.45	0.97
A65	5.70	97	5.26	0.87
A66	5.80	99	6.00	0.87
A67	5.62	96	7.22	1.03

Electronic Measurements

Before discussing the electronic properties of the materials, some definitions are required. The dielectric constant of a given material can be related to the amount of energy storage by measuring the capacitance (F) of the material, where $\varepsilon = C(F)xd/\varepsilon_0 A$, d = thickness, A = area, and $\varepsilon_0 = 8.8542 \times 10^{-12}$ F/m. In general, for any given material the dielectric constant $\varepsilon = \varepsilon' - i\varepsilon''$. The loss tangent (tan δ) of the material is related to the energy dissipated and is given by the ratio of the imaginary part of the dielectric constant ε'' divided by the real part ε'. The Curie temperatures, dielectric constants, ε', and % tunability was determined at the ARL-Microwave and Photonics Branch Electronic Power Sources Directorate. The tunability of a material is defined as:

$$\% \text{ tunability} = (\varepsilon(0) - \varepsilon(V_{app}))/(\varepsilon(0)). \quad (1)$$

The block diagram of the experimental apparatus for measuring the tunability, dielectric constants, Curie temperature, and hysterisis is shown in Figure 1. The sample is encapsulated in a dry box and is heated and cooled with a thermoelectric cooler (TEC). The TEC has two wires connected to the computer controlled by a double throw switch which changes the polarity of the voltage applied to the TEC. The temperature is held within $\pm$ 0.05°C. The device under test (DUT) is painted on both sides with silver epoxy and mounted to the brass plate holder with epoxy. A wire is fixed to the top of the specimen and held in place with a Teflon^{TM} plate, and tightened with two tension screws, as shown in Figure 2. The fixture is placed in an oven at 150°C for one hour to anneal the silver epoxy; then, the specimen is placed into a dry box and the test is run. The data includes standard deviation at each point. The tunability measurements were taken with an applied electric field which ranged from 0 V/micron to 1.5 V/micron. All of the electronic properties reported here were measured at a frequency of 1 KHz.

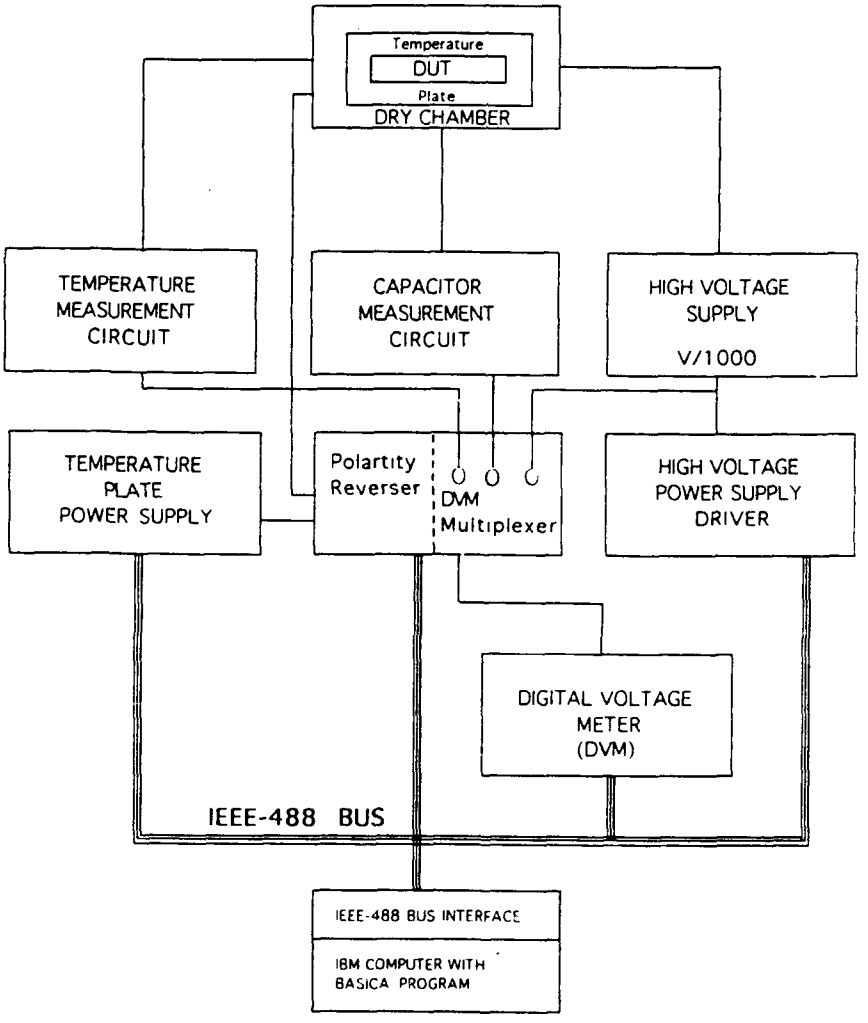

Figure 1 Block diagram of ARL-EPSD electronic test equipment.

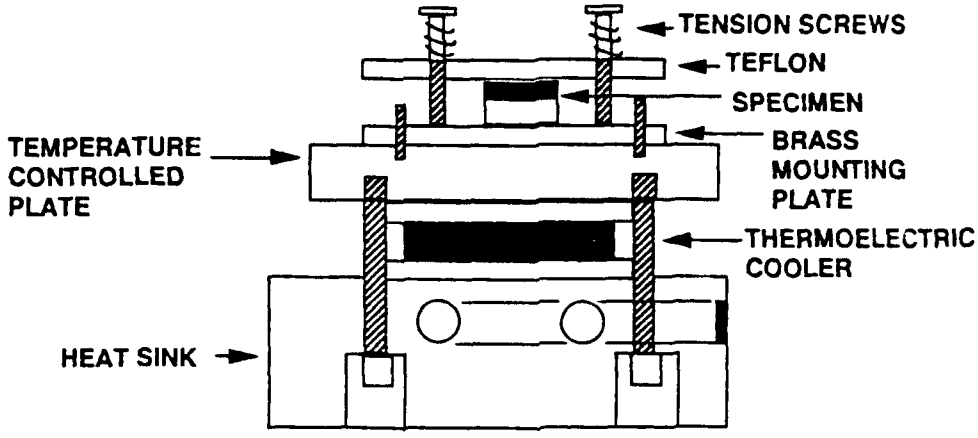

Figure 2. Specimen holder and heating apparatus for electronic test system

Results and Discussion

The inverse of the dielectric constant versus temperature for samples A68 and A30 are shown in Figures 3(a) and 3(b). The degree of homogeneity in the materials can be determined from how well the data obeys the Curie-Weiss law, where:

$$1/\varepsilon = 1/\varepsilon_0 \left((T-T_c)/(T+2T_c)\right), \quad (2)$$

T_c = Curie temperature, $\varepsilon_0 = 8.8542 \times 10^{-12}$ F/m.

Using the data shown in Figure 3, the relationship described by Equation 2 is followed until 2°C of the Curie temperature (40°C). This indicates that the sample is highly uniform and that the dielectric properties of the bulk are representative of the entire specimen.

Dopants in BSTO (Ba=0.75)

A summary of the electronic properties of the doped BSTO (Ba=0.75) specimens is given in Table 3. The specimens were measured at 1 KHz and the electric field was increased to 1.5 V/μm. Dopants that were studied in this investigation either substitute for the Ba site or the Ti site in the material. Generally, the dopants, which are compounds, will have constituents that will predominantly substitute into these lattice positions. The effects of these substitutions are: if substituted into the Ba site to shift the Curie temperature, or if substituted into the Ti site to suppress the Curie temperature. Compound dopants ultimately occupy integranular positions and do not combine totally into the lattice positions. Therefore, studying the electronic behavior can indicate the subtle effect of the dopants on the crystal structure of the materials even if the lattice parameters and X-ray diffraction patterns are not affected. To clarify the differences between the effect of the dopant and that of Sr in the ceramics, identical dopants have been added to barium titanate

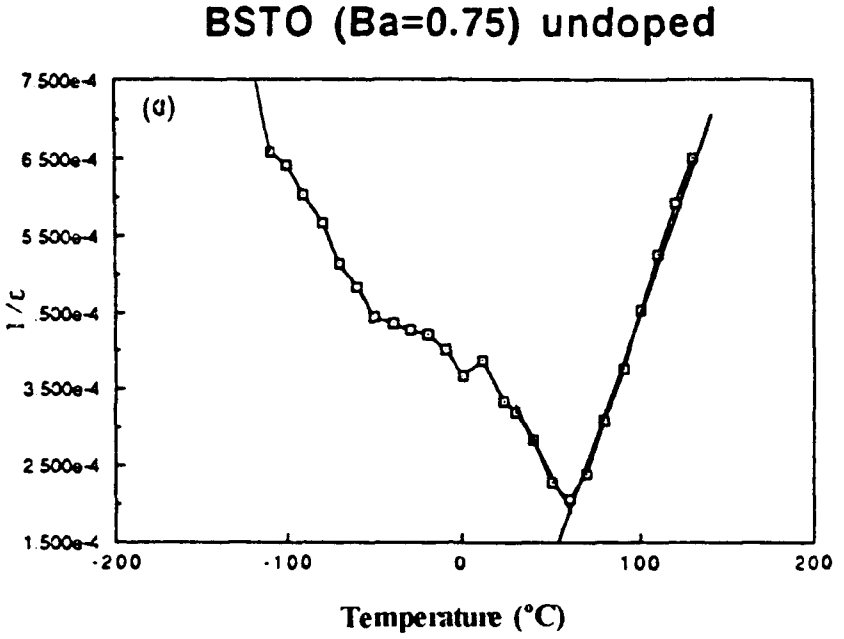

(a)

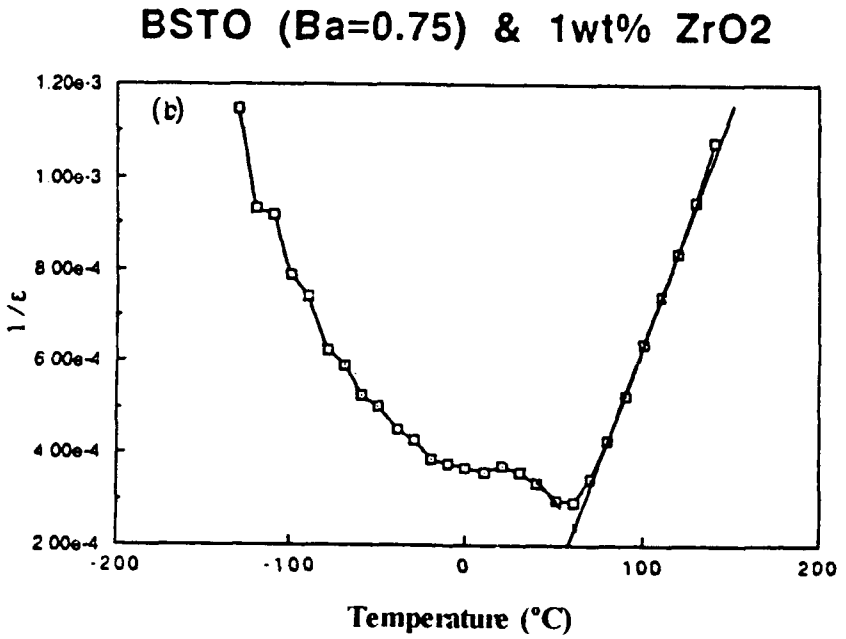

(b)

Figure 3. Curie-Weiss relationship $1/\varepsilon$ versus temperature for: (a) an undoped specimen, and (b) a specimen doped with 2 wt% zirconia.

Table 2 Electronic properties of doped BSTO (Ba=0.75) measured at 1 KHz

Sample #	Dielectric constant	Curie temperature (°C)	Tunability (%)	Hysteresis (%)
A30	1630	60	28.0	2.0
A31	1388	55	27.0	2.0
A32	1193	54	23.0	0.2
A33	549	-60	1.5	0.2
A35	675	55	17.0	—
A36	474	60	17.0	2.0
A38	532	40	23.0	0.3
A39	930	50	28.0	0.6
A40	25	–	4.0	0.1
A68	1150	60	32.0	5.0

For a clearer understanding of the trends found in the results, some of the data will be presented in a graphic format, as shown in Figures 4 and 5. It is obvious from these figures (Figure 4 shows the dielectric constant versus tunability and Figure 5 shows the Curie temperature versus tunability) that the tunability increases with increasing dielectric constant and also with increasing Curie temperature. This is a direct consequence of the fact that the tunability is greatest at the peak of the Curie temperature and is also high at temperatures below the Curie point where the material is in the *ferroelectric* region. At temperatures far above the Curie temperature (in the *paraelectric* region) for a particular composition the tunability drops off rapidly. Likewise, the dielectric loss of any given material is decreased when the material is measured in its paraelectric region or, in other words, when the Curie temperature is decreased. This was observed for sample A30 (1 wt% zirconia) which had a loss tangent of 0.36 at 10 GHz (Curie temperature of 60°C, dielectric constant = 1630) as compared to sample A31 which was doped with 1 wt% zirconia and 1 wt% $BaLiF_3$ (Curie temperature of 55°C, dielectric constant = 1388) and has a loss tangent of 0.15. As seen above, the loss tangent seems to decrease with dielectric constant. A30 and A31 can be compared to A39 (doped with 30 wt% alumina) which at 39 GHz has a dielectric constant of 45.8 and a loss tangent of 0.054. The loss tangent is definitely less for the lower dielectrics. It should be noted that compositions which had Curie temperatures below room temperature had a tunability of less than 10%. The % hystersis is not directly related to changes in the dielectric properties. However, in the paraelectric region the hysteresis is thought to be due to aging under bias.

The grain size of the material is related to the electronic properties, as can be seen in Figure 6. As the grain size decreases, the dielectric constant increases in these materials and the increase reaches a maximum at grain sizes of around 10 microns. This behavior has been noted previously and has been attributed to an increase in the domain width and increase in internal stress below a critical grain size (2). Figure 7 shows the tunability and the Curie temperature versus grain size. As expected, below a critical grain size of about 1 micron both the tunability and Curie temperature decrease drastically.

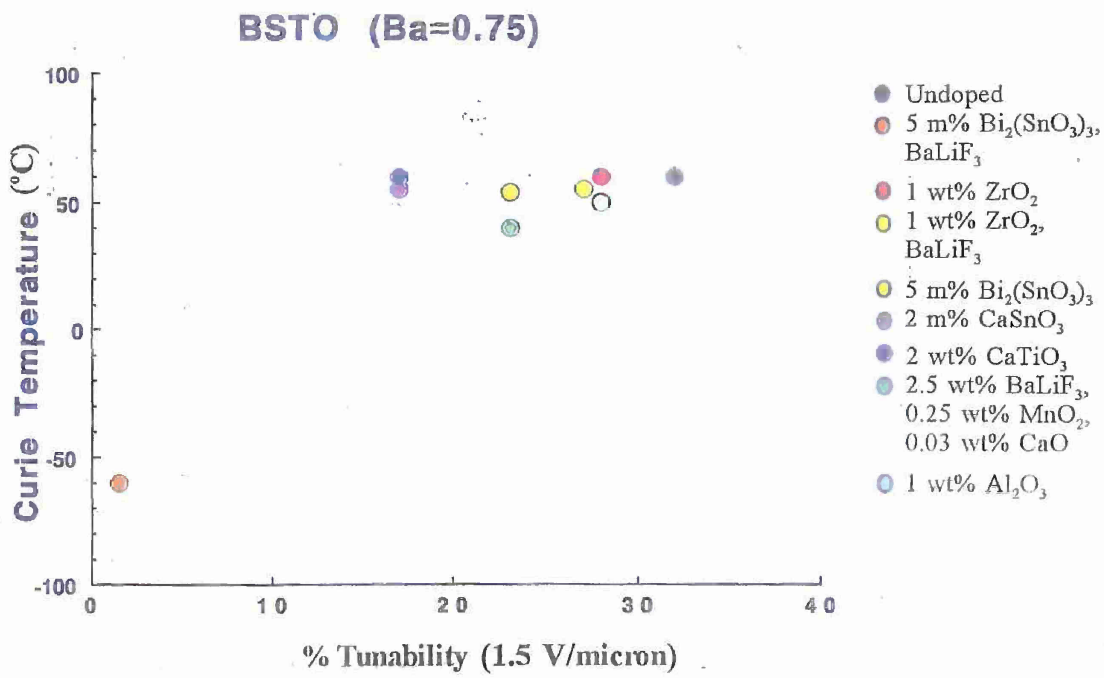

Figure 4. Dielectric constant versus tunability (1.5 V/micron) for doped BSTO (Ba=0.75).

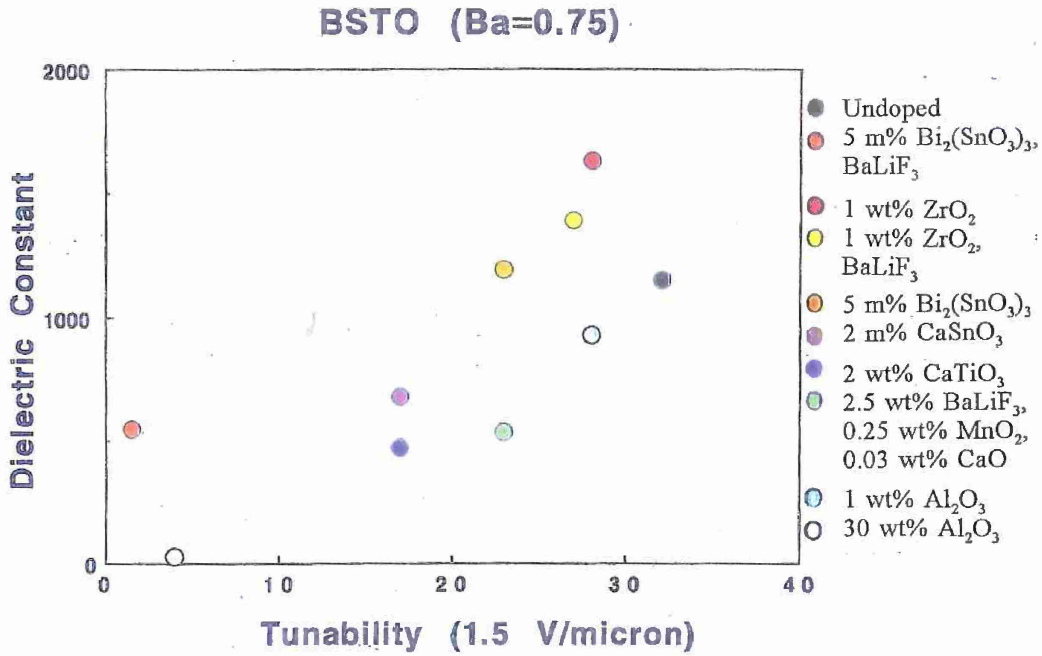

Figure 5. Curie temperature (°C) versus % tunability (1.5 V/micron) for doped BSTO (Ba=0.75).

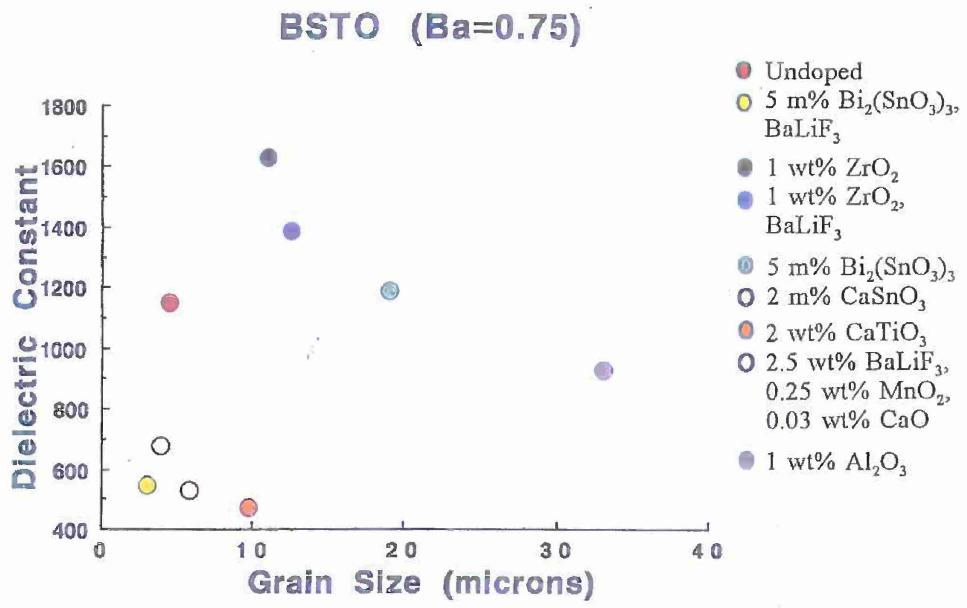

Figure 6. Dielectric constant versus grain size for doped BSTO (Ba=0.75).

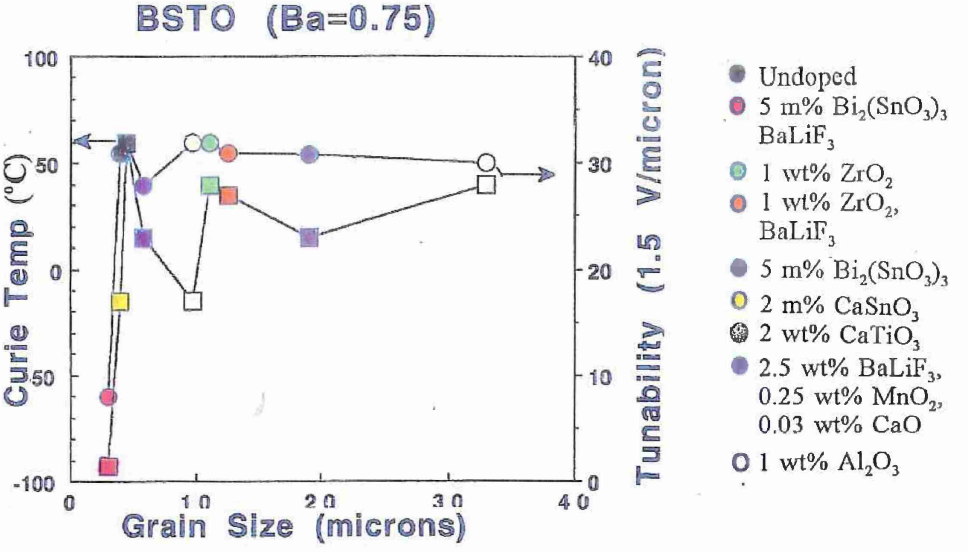

Figure 7. Curie temperature and tunability (1.5 V/micron) versus grain size for doped BSTO (Ba=0.75).

Dopants in BTO

The results of the electronic properties of BTO doped with the identical dopants of the BSTO samples are shown in Table 4. As shown in Figures 8 and 9, similar results are shown for the dopants when added to BTO. As expected, the tunability, in general, is less than the BSTO (Ba=0.75) samples; this is because the Curie temperature of undoped barium titanate is very much above room temperature (120°C). The primary reason strontium is used is the fact that controlling the Curie temperature is the most effective method for controlling tunability. As obtained for the doped BSTO (Ba=0.75) materials, the tunability decreases when any dopant is added to pure barium titanate. Also, similar to BSTO, the doped BTO samples with the lowest tunabilities (samples A59 and A67) have the lowest Curie temperatures which are below room temperature. This, again, leads to the conclusion that when operating these ferroelectric materials in the paraelectric region the tunability is decreased. However, as shown in Table 4, and as stated before, the loss is also decreased (these losses are approximate values). However, the dielectric constant does not increase with an increase in tunability and is not clearly related to the tunability as in the case of BSTO. This is probably because of the differences in the Curie temperature in the case of BSTO as compared to BTO. In the case of BSTO (Ba=0.75), the peak of the dielectric constant (40°C) is near to the operating (room) temperature; therefore, small variations in the position on this curve make a large difference in the value obtained for the dielectric constant as well as in the tunability. On the other hand, for BTO (Curie temperature = 120°C) at room temperature, the dielectric constant curve is fairly flat. Small changes in the dielectric cannot greatly affect the tunability. Also, the magnitude of the change in the dielectric is not as great as that experienced with the BSTO samples.

Table 4. Electronic properties of doped BTO measured at 1 KHz

Sample #	Dielectric constant	Curie temperature (°C)	Tunability (%)	Tan δ
A58	814	110	17.0	0.100
A59	575	-70	0.8	0.010
A60	14	40	1.0	0.010
A61	880	130	10.0	0.100
A62	1267	100	13.0	0.010
A63	1617	130	8.0	0.010
A64	695	135	3.0	0.010
A65	97	90	5.0	0.010
A67	410	-50	0.4	0.010
A69	952	120	22.0	0.100

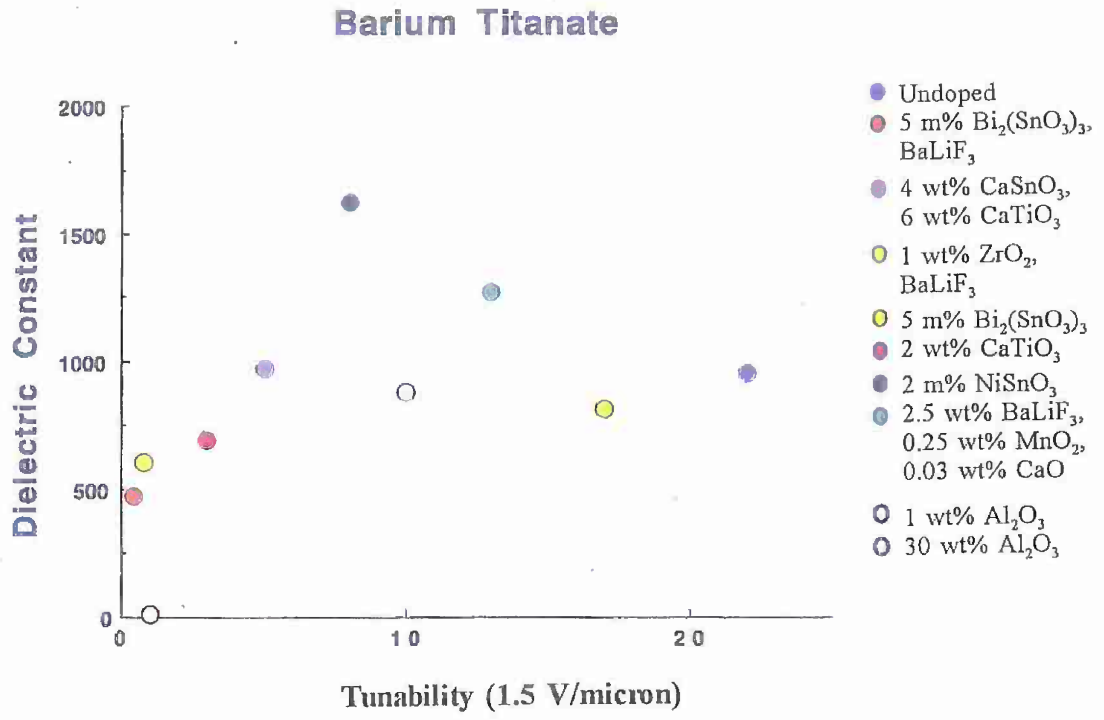

Figure 8. Dielectric constant versus tunability (1.5 V/micron) for doped BTO.

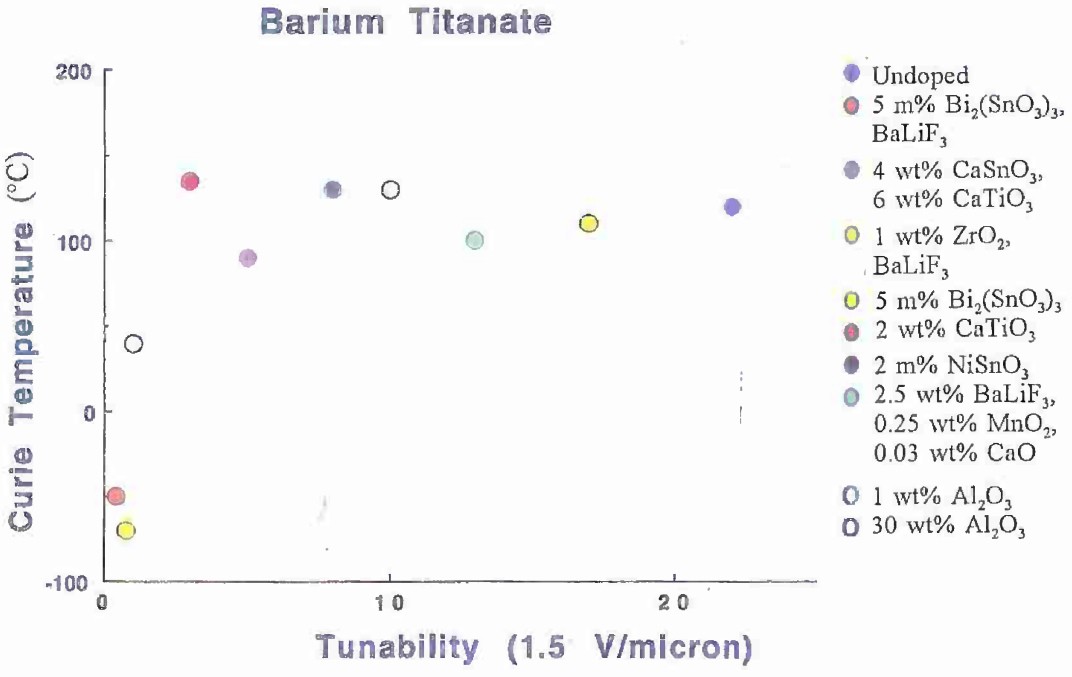

Figure 9. Curie temperature (°C) versus % tunability (1.5 V/micron) for doped BTO.

The grain size versus dielectric constant of the doped BTO samples are shown in Figure 10. As seen in the case of the doped BSTO samples, the dielectric increases with the decrease in grain size until about 1 μm. This result has been reported previously and was attributed to the decrease in domain width and the increase in internal stress (2). The grain size below, which the dielectric begins to decrease, is less in the case of BTO as compared to BSTO. As shown in Figure 11, the tunability and

THIS
PAGE
IS
MISSING
IN
ORIGINAL
DOCUMENT

Curie temperature decrease rapidly below a grain size of 1 micron, which was the case for BSTO. This produced investigation of the grain size and the electronic properties as a function of Ba(1-x) content in the material which will be discussed in the following section.

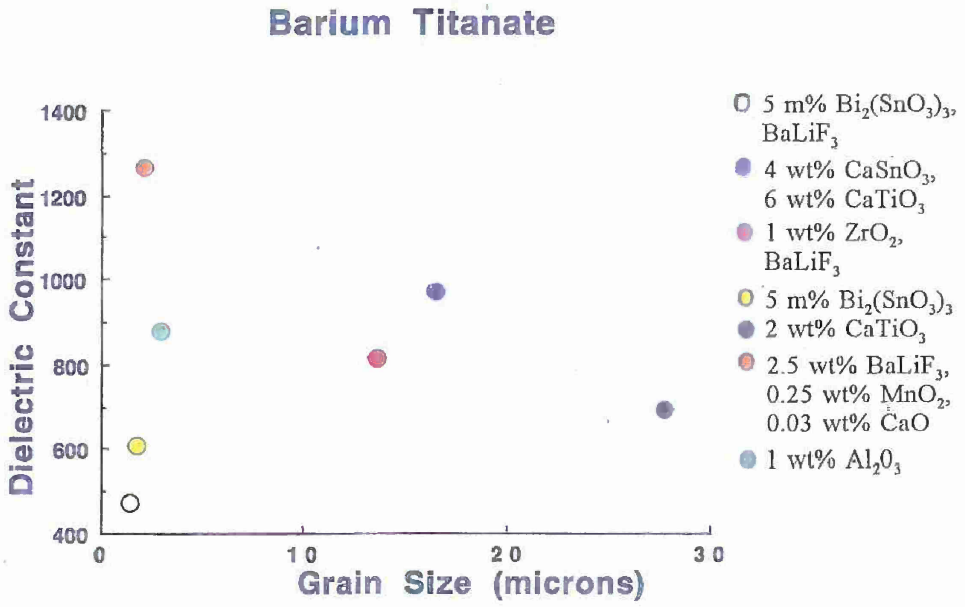

Figure 10. Dielectric constant versus grain size for doped BTO.

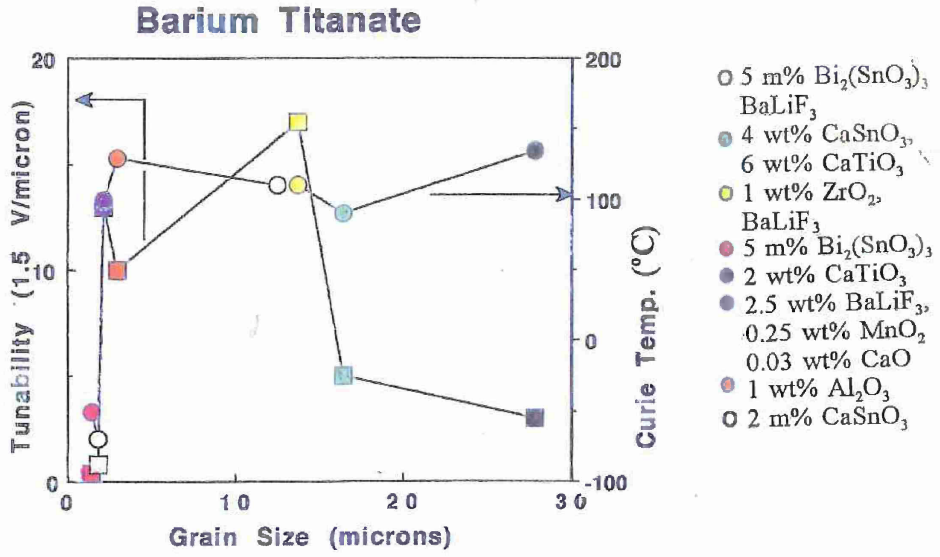

Figure 11. Curie temperature and tunability (1.5 V/micron) versus grain size for doped BTO.

Variation of Ba(1-x) Content in Undoped and Doped BSTO

As shown in Figure 12, the dielectric constant is a maximum at barium content between 1-x = 0.65 to 0.70. This is because these compositions have Curie temperatures which are at room temperature and, therefore, represent peak dielectric constants for the material. Figure 13 shows the tunability versus Ba(1-x) content. The tunability is also a maximum for compositions in the range from 1-x = 0.65 to 0.75. Again, this is due to the temperature at which the peak dielectric constant occurs which is, for these compositions, around room temperature. Since the tunability is essentially the derivative with respect to voltage of the dielectric constant curve, the maximum tunability should occur at the steepest point of the curve which is at room temperature for those compositions. The Curie temperature versus composition (Ba(1-x)) is shown in Figure 14. As displayed in Figure 14, the relationship is linear. This linearity and controllability is due to the fact that the addition of strontium changes the phase of the material from tetragonal at room temperature for barium titanate to cubic at room temperature for BSTO, with a linear decrease in the lattice constant as the strontium content is increased. Since the addition of strontium offers this very linear and controlled modification of the Curie temperature in barium titanate, it has been a widely used additive and is commonly used in the capacitor industry.

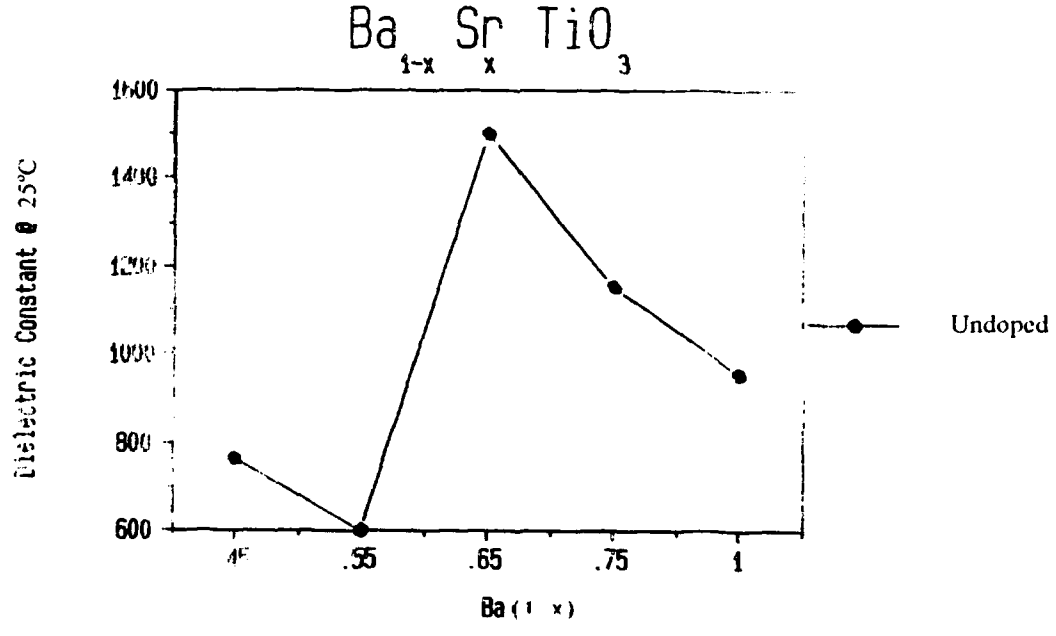

Figure 12. Dielectric constant versus barium content, (Ba(1-x), for undoped materials.

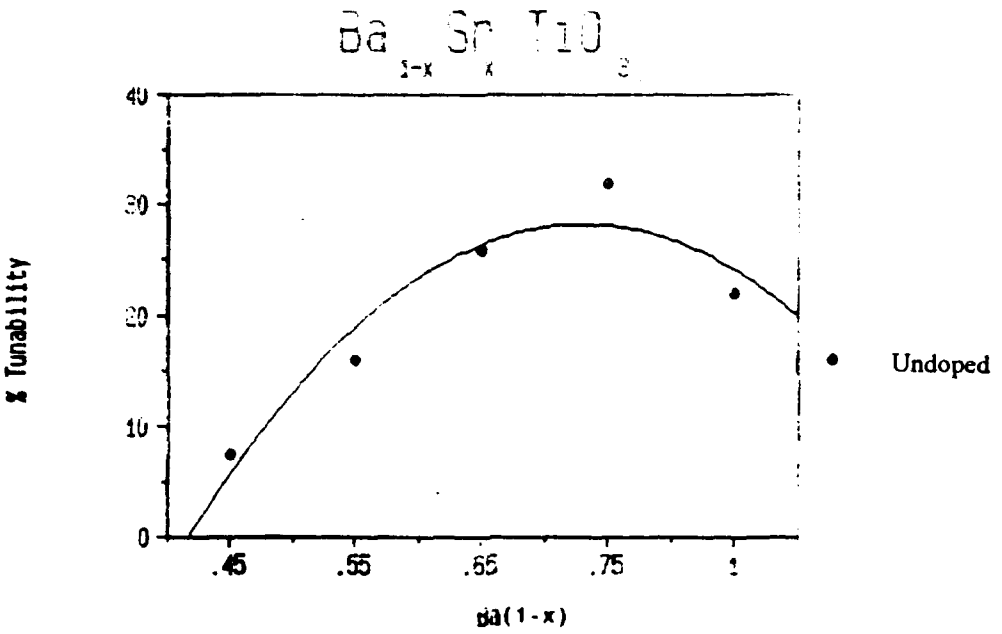

Figure 13. Tunability (%, 1.5 V/micron) versus barium content, Ba(1-x), for undoped materials.

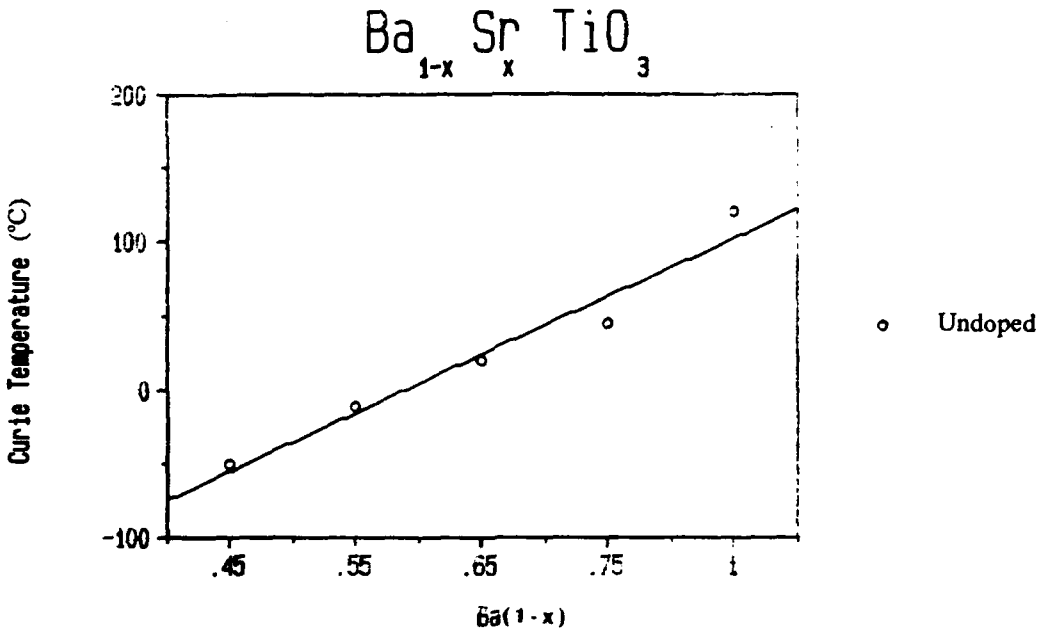

Figure 14. Curie temperature versus barium content, Ba(1-x), for undoped materials.

Figures 15, 16, and 17 show the relationship between the dielectric constant, tunability, Curie temperature, and barium content for specimens doped with $BaLiF_3$. The relationships of the electronic properties (dielectric, constant, Curie temperature, and tunability) versus Sr composition are unchanged when other dopants such as $BaLiF_3$ is added to the material. The electronic properties versus Ba(1-x) content are also unchanged for ZrO_2 samples. This indicates that these other dopants, at the levels incorporated, have little affect on the lattice constants and crystal structure of the material.

This was indeed found from the X-ray diffraction data which did not show any change in the lattice constants (compared to the undoped materials with the same Sr content). The dopants, however, do decrease the tunability and, in the case of the fluoride dopants, the dielectric constant is decreased. Zirconia at this level of substitution does not decrease the dielectric constant.

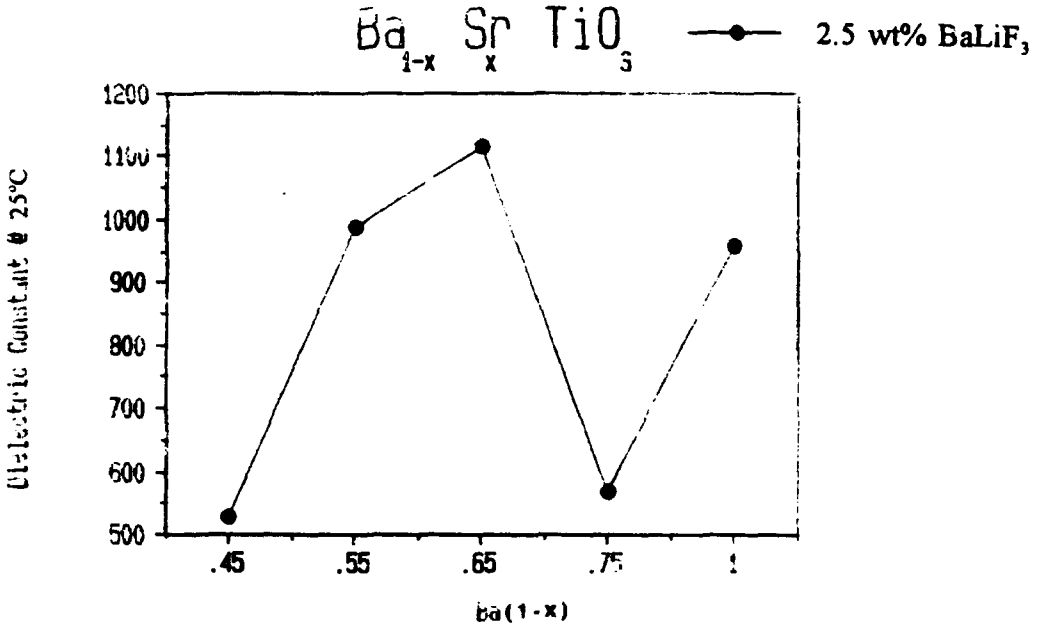

Figure 15. Dielectric constant versus barium content, Ba(1-x), for materials doped with 2.5 wt% $BaLiF_3$.

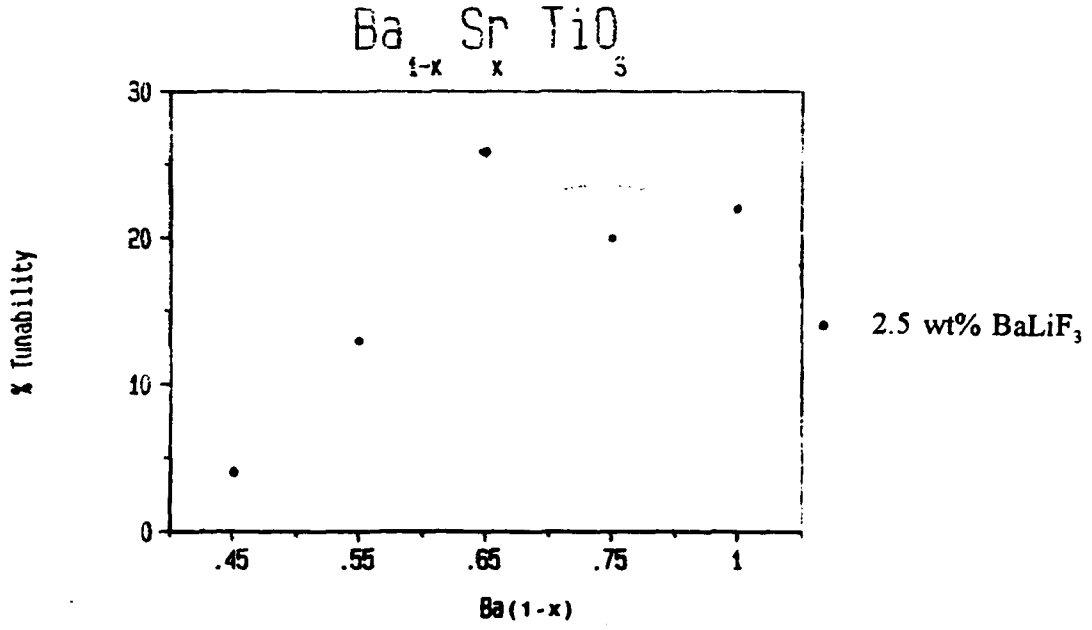

Figure 16. Tunability (%, 1.5 V/micron) versus barium content, Ba(1-x), for materials doped with 2.5 wt% $BaLiF_3$.

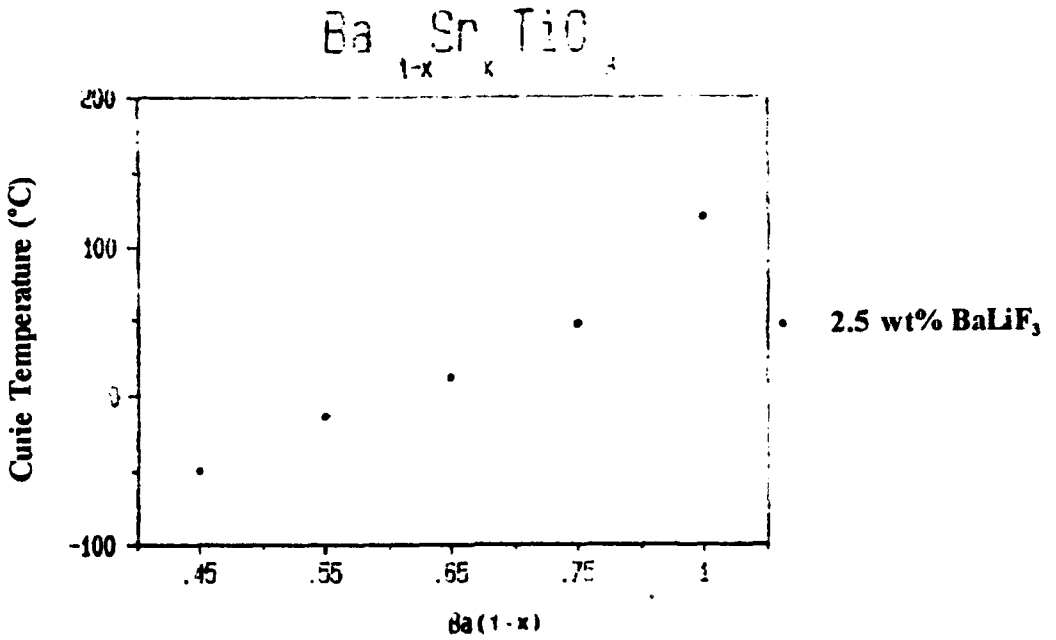

Figure 17. Curie temperature versus barium content, Ba(1-x), for materials doped with 2.5 wt% $BaLiF_3$.

Figure 18 shows the Ba(1-x) content and dielectric constant versus grain size for undoped specimens. As seen in the figure, the grain size increases with the increase in Ba(1-x) content, which is as expected. However, the dielectric constant increases with the decrease in grain size, which indicates a maximum dielectric constant at a grain size of about 10 microns (composition of about Ba(1-x) = 0.65). Then, the dielectric constant decreases with further decrease in grain size below 10 microns. The decrease in dielectric constant is probably due to the shift in Curie temperature, as well as grain size effects.

Figure 19 shows the grain size versus Ba(1-x) content for doped BSTO with 1 wt% ZrO_2 as compared to the undoped specimens. It is obvious that the addition of zirconia decreases the grain size. The data does indicate a slight decrease in the dielectric constant for compositions where the grain size is also the most dramatically affected; i.e., for barium content = 1.00, 0.75, and 0.65. However, specimens with varying barium content doped with zirconia showed identical trends in the dielectric constant and other electronic properties versus barium content as the undoped and the specimens doped with $BaLiF_3$. This is probably because zirconia does effect the Curie temperature as does the strontium titanate; therefore, the change in the dielectric constant with the change in the barium content is the dominant effect at this level of zirconia substitution. The substitution of zirconia does broaden the Curie temperature and decreases the dielectric constant for compositions which are in the ferroelectric region, and this broadening effects room temperature dielectric constant data.

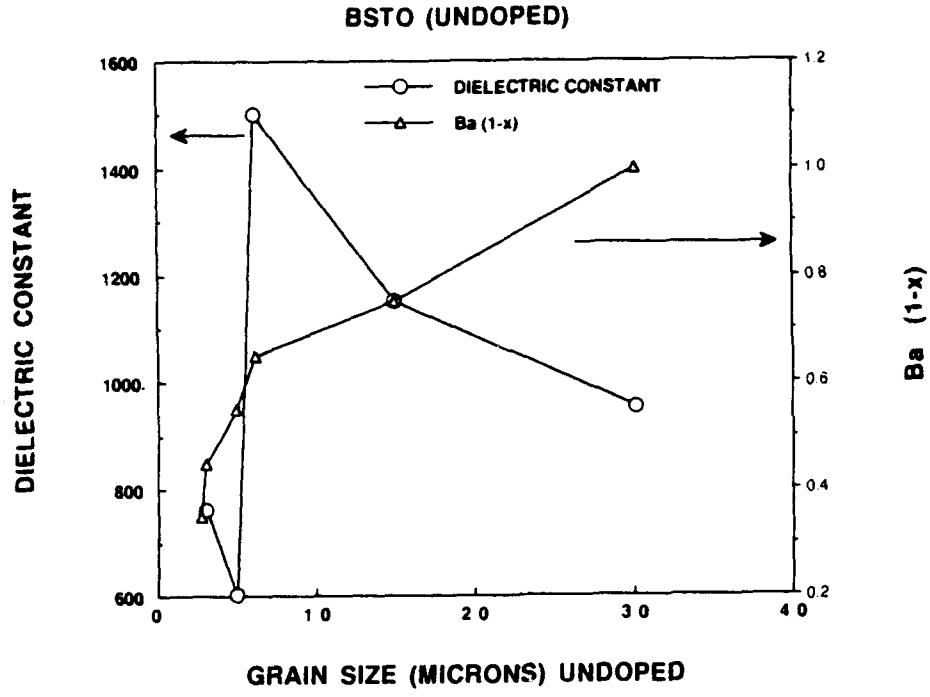

Figure 18. Barium content, Ba(1-x), and dielectric constant versus grain size for undoped materials.

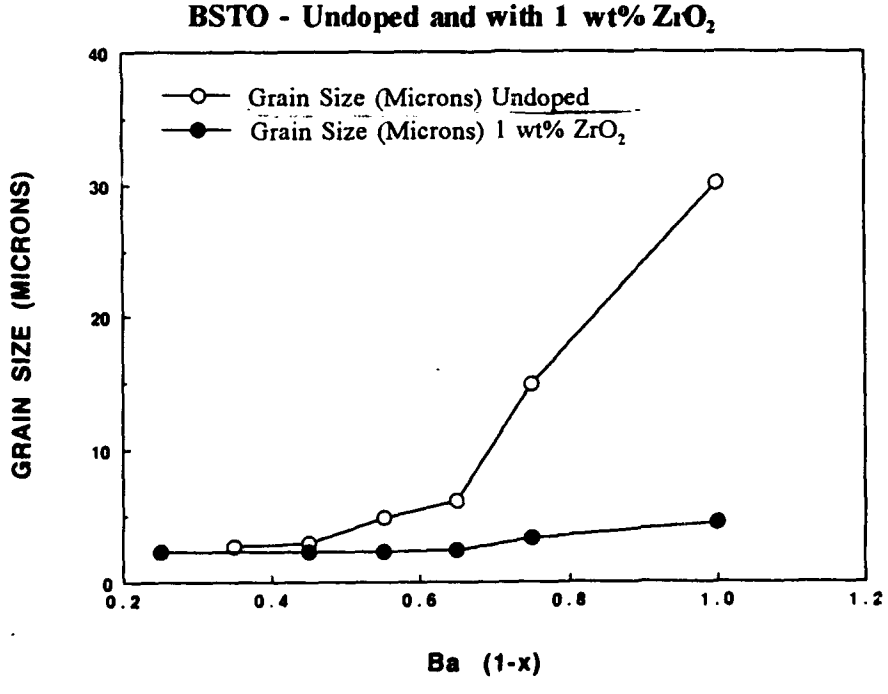

Figure 19. Barium content, Ba(1-x), versus grain size for undoped materials and materials doped with 1.0 wt% zirconia.

Conclusions

For dopant modifications BSTO (Ba(1-x) = 0.75) as studied in this investigation, it was found that the tunability increases with an increase in the dielectric constant and with an increase in Curie temperature. The tunability, however, is the greatest in the undoped material. The loss tangent (10 GHz) was also found to increase with an increase in the Curie temperature. This is because the loss tangent is the greatest when the material is in the ferroelectric phase; therefore, it is the greatest for materials which have Curie temperatures at and above room temperature.

BTO with the same additives as used in the above mentioned portion of this investigation shows similar electronic behavior. The tunability obtained for these specimens even in the undoped specimen is less than in the BSTO (0.75) samples. Also, the dopants again reduce the tunability as compared to the undoped BTO specimen. The dielectric constant is not as clearly related to the tunability as in the BSTO materials. This is because the Curie temperature of almost all of these samples are far above room temperature.

Variation of the barium content shows that the maximum tunability and dielectric constant occur at a barium content Ba(1-x) = 0.65. This is because this composition has a Curie temperature at room temperature. Therefore, the peak dielectric constant and the room temperature dielectric constant coincide. Also, the Curie temperature increases linearly with an increase in barium content. $BaLiF_3$ and ZrO_2 at the levels incorporated in this study do not change the relationships described above.

The grain size is related to the electronic properties. For the doped BSTO (0.75) specimens, the dielectric constant increases with a decrease in grain size; then, beyond a critical grain size of 10 microns the dielectric constant decreases. Similar behavior was found in the doped BTO specimens. The grain size of the specimens decreases with the decrease in barium content and also when zirconia is added. The zirconia doped materials show less of a dependence on barium content. In order to further clarify relationships between microstructures and electronic properties, various amounts of the same dopant will be added to a single composition of BSTO. However, it is clear that the grain size plays an important role in controlling the electronic properties of the BSTO, and the grain size seems to effect all of the electronic properties simultaneously.

Acknowledgments

The authors would like to thank the engineers of Transelco Division of Ferro Corporation in particular Jim Henry and Jim Wilson for their kind donations of advice and materials.

References

1. BABBITT, R. W., KOSCICA, T. E., and DRACH, W. E. Microwave Journal, v. 35, 1992, p. 63.
2. ARLT, G., HENNINGS, D., and deWITH, G. J. Appl. Phys., v. 58, 1985, p. 1619.

DISTRIBUTION LIST

No. of Copies	To
1	Office of the Under Secretary of Defense for Research and Engineering, The Pentagon, Washington, DC 20301
	Director, U.S. Army Research Laboratory, 2800 Powder Mill Road, Adelphi, MD 20783-1197
1	ATTN: AMSRL-OP-CI-AD, Technical Publishing Branch
1	AMSRL-OP-CI-AD, Records Management Administrator
	Commander, Defense Technical Information Center. Cameron Station, Building 5, 5010 Duke Street, Alexandria, VA 23304-6145
2	ATTN: DTIC-FDAC
1	MIA/CINDAS, Purdue University, 2595 Yeager Road, West Lafayette, IN 47905
	Commander, Army Research Office, P.O. Box 12211, Research Triangle Park, NC 27709-2211
1	ATTN: Information Processing Office
	Commander, U.S. Army Materiel Command, 5001 Eisenhower Avenue, Alexandria, VA 22333
1	ATTN: AMCSCI
	Commander, U.S. Army Materiel Systems Analysis Activity, Aberdeen Proving Ground, MD 21005
1	ATTN: AMXSY-MP, H. Cohen
	Commander, U.S. Army Missile Command, Redstone Arsenal, AL 35809
1	ATTN: AMSMI-RD-CS-R/Doc
	Commander, U.S. Army Armament, Munitions and Chemical Command, Dover, NJ 07801
2	ATTN: Technical Library
	Commander, U.S. Army Natick Research, Development and Engineering Center, Natick, MA 01760-5010
1	ATTN: Technical Library
	Commander, U.S. Army Satellite Communications Agency, Fort Monmouth, NJ 07703
1	ATTN: Technical Document Center
	Commander, U.S. Army Tank-Automotive Command, Warren, MI 48397-5000
1	ATTN: AMSTA-ZSK
1	AMSTA-TSL, Technical Library
	Commander, White Sands Missile Range, NM 88002
1	ATTN: STEWS-WS-VT
	President, Airborne, Electronics and Special Warfare Board, Fort Bragg, NC 28307
1	ATTN: Library
	Director, U.S. Army Research Laboratory, Weapons Technology, Aberdeen Proving Ground, MD 21005-5066
1	ATTN: AMSRL-WT

No. of Copies	To
	Commander, Dugway Proving Ground, UT 84022
1	ATTN: Technical Library, Technical Information Division
	Commander, U.S. Army Research Laboratory, 2800 Powder Mill Road, Adelphi, MD 20783
1	ATTN: AMSRL-SS
	Director, Benet Weapons Laboratory, LCWSL, USA AMCCOM, Watervliet, NY 12189
1	ATTN: AMSMC-LCB-TL
1	AMSMC-LCB-R
1	AMSMC-LCB-RM
1	AMSMC-LCB-RP
	Commander, U.S. Army Foreign Science and Technology Center, 220 7th Street, N.E., Charlottesville, VA 22901-5396
3	ATTN: AIFRTC, Applied Technologies Branch, Gerald Schlesinger
	Commander, U.S. Army Aeromedical Research Unit, P.O. Box 577, Fort Rucker, AL 36360
1	ATTN: Technical Library
	U.S. Army Aviation Training Library, Fort Rucker, AL 36360
1	ATTN: Building 5906-5907
	Commander, U.S. Army Agency for Aviation Safety, Fort Rucker, AL 36362
1	ATTN: Technical Library
	Commander, Clarke Engineer School Library, 3202 Nebraska Ave., N, Fort Leonard Wood, MO 65473-5000
1	ATTN: Library
	Commander, U.S. Army Engineer Waterways Experiment Station, P.O. Box 631, Vicksburg, MS 39180
1	ATTN: Research Center Library
	Commandant, U.S. Army Quartermaster School, Fort Lee, VA 23801
1	ATTN: Quartermaster School Library
	Naval Research Laboratory, Washington, DC 20375
2	ATTN: Dr. G. R. Yoder - Code 6384
	Chief of Naval Research, Arlington, VA 22217
1	ATTN: Code 471
	Commander, U.S. Air Force Wright Research & Development Center, Wright-Patterson Air Force Base, OH 45433-6523
1	ATTN: WRDC/MLLP, M. Forney, Jr.
1	WRDC/MLBC, Mr. Stanley Schulman
	U.S. Department of Commerce, National Institute of Standards and Technology, Gaithersburg, MD 20899
1	ATTN: Stephen M. Hsu, Chief, Ceramics Division, Institute for Materials Science and Engineering

No. of Copies	To
1	Committee on Marine Structures, Marine Board, National Research Council, 2101 Constitution Avenue, N.W., Washington, DC 20418
1	Materials Sciences Corporation, Suite 250, 500 Office Center Drive, Fort Washington, PA 19034
1	Charles Stark Draper Laboratory, 555 Technology Square, Cambridge, MA 02139
	Wyman-Gordon Company, Worcester, MA 01601
1	ATTN: Technical Library
	General Dynamics, Convair Aerospace Division, P.O. Box 748, Fort Worth, TX 76101
1	ATTN: Mfg. Engineering Technical Library
	Plastics Technical Evaluation Center, PLASTEC, ARDEC, Bldg. 355N, Picatinny Arsenal, NJ 07806-5000
1	ATTN: Harry Pebly
1	Department of the Army, Aerostructures Directorate, MS-266, U.S. Army Aviation R&T Activity - AVSCOM, Langley Research Center, Hampton, VA 23665-5225
1	NASA - Langley Research Center, Hampton, VA 23665-5225
	U.S. Army Vehicle Propulsion Directorate, NASA Lewis Research Center, 2100 Brookpark Road, Cleveland, OH 44135-3191
1	ATTN: AMSRL-VP
	Director, Defense Intelligence Agency, Washington, DC 20340-6053
1	ATTN: ODT-5A (Mr. Frank Jaeger)
	U.S. Army Communications and Electronics Command, Fort Monmouth, NJ 07703
1	ATTN: Technical Library
	U.S. Army Research Laboratory, Electronic Power Sources Directorate, Fort Monmouth, NJ 07703
1	ATTN: AMSRL-EP-M, W. C. Drach
1	AMSRL-EP-M, T. E. Koscica
1	AMSRL-EP-M, R. W. Babbit
	Director, U.S. Army Research Laboratory, Watertown, MA 02172-0001
2	ATTN: AMSRL-OP-CI-D, Technical Library
20	Authors